Progress In Electromagnetics Research, PIER 81, 393–412, 2008

NUMERICAL APPROACH TO SURVEY THE PROBLEM OF ELECTROMAGNETIC SCATTERING FROM RESISTIVE STRIPS BASED ON USING A SET OF ORTHOGONAL BASIS FUNCTIONS

S. Hatamzadeh-Varmazyar

Department of Electrical Engineering
Islamic Azad University
Science and Research Branch, Tehran, Iran

M. Naser-Moghadasi

Central Commission for Scientific
Literacy & Art Societies
Islamic Azad University
Science and Research Branch, Tehran, Iran

E. Babolian

Department of Mathematics
Teacher Training University
599 Taleghani Avenue, Tehran 15618, Iran

Z. Masouri

Department of Mathematics
Islamic Azad University
Science and Research Branch, Tehran, Iran

Abstract——In this paper, the problem of electromagnetic scattering from resistive strips is solved and discussed. This problem is modeled by the integral equations of the second kind. The basic mathematical concept is collocation method using block-pulse orthogonal basis functions. An effective numerical method for solving these integral equations is proposed. The problem of electromagnetic scattering from resistive strips is treated in detail, the illustrative computations are given for several cases, and an extensive discussion on the obtained results is performed. This method can be generalized to apply to objects of arbitrary geometry.

1. INTRODUCTION

The development of numerical methods for solving integral equations in Electromagnetics has attracted intensive researches for more than four decades [1, 2]. The use of high-speed computers allows one to make more computations than ever before. During these years, careful analysis has paved the way for the development of efficient and effective numerical methods and, of equal importance, has provided a solid foundation for a through understanding of the techniques.

Over several decades, electromagnetic scattering problems have been the subject of extensive researches (see [3–42]). Scattering from arbitrary surfaces such as square, cylindrical, circular, spherical [3–9] are commonly used as test cases in computational Electromagnetics, because analytical solutions for scattered fields can be derived for these geometries [3].

An important parameter in scattering studies is the electromagnetic scattering by a target which is usually represented by its *echo area* or *radar cross section* (RCS) [43]. The echo area or RCS is defined as the area intercepting the amount of power that, when scattered isotropically, produces at the receiver a density that is equal to the density scattered by the actual target [44]. For a two-dimensional target the scattering parameter is referred to as the *scattering width* (SW) or alternatively as the *radar cross section per unit length*.

When the transmitter and receiver are at the same location, the RCS is usually referred to as *monostatic* (*or backscattered*) and it is referred to as *bistatic* when the two are at different locations [43]. Observations made toward directions that satisfy Snell's law of reflection are usually referred to as specular. Therefore the RCS of target is very important parameter which characterizes its scattering properties. A plot of the RCS as a function of the space coordinates is usually referred to as the RCS pattern.

Determining the scattered electromagnetic fields from resistive strips leads to solve the integral equations of the second kind with complex kernels. Of course, if the resistance of the strip approaches to zero, then the problem is modeled by integral equations of the first kind. However, for solving integral equations of the second kind, several numerical approaches have been proposed. These numerical methods often use the basis functions and transform the integral equation to a linear system that can be solved by direct or iterative methods [45]. It is important in these methods to select an appropriate set of basis functions so that the approximate solution of integral equation has a good accuracy.

It is the purpose of this paper to use the block-pulse functions

(BPFs) as a set of orthogonal basis functions and to apply them to the collocation method for determining the scattered electromagnetic fields from resistive strips. Using this method, the second kind integral equation reduces to a linear system of algebraic equations. Solving this system gives an approximate solution for these problems.

First of all, some characteristics of BPFs are described. Then the collocation method is proposed for solving integral equations of the second kind using BPFs. The problem of electromagnetic scattering from resistive strips is described in detail and solved by the presented method. Also, the illustrative computations are given for several cases. Finally, an extensive discussion on the obtained results is performed.

2. BLOCK-PULSE FUNCTIONS

One very important step in any numerical solution is the choice of basis functions.

Block-pulse functions (BPFs) have been studied by many authors and applied for solving different problems; for example, see [46, 47].

2.1. Definition

An m-set of BPFs is defined over the interval $[0, T)$ as [46]:

$$\phi_i(t) = \begin{cases} 1, & \dfrac{iT}{m} \leqslant t < \dfrac{(i+1)T}{m}, \\ 0, & \text{otherwise}, \end{cases} \tag{1}$$

where $i = 0, 1, \ldots, m-1$ with a positive integer value for m. Also, consider $h = T/m$, and ϕ_i is the ith BPF.

There are some properties for BPFs, the most important properties are disjointness, orthogonality, and completeness.

The disjointness property can be clearly obtained from the definition of BPFs:

$$\phi_i(t)\phi_j(t) = \begin{cases} \phi_i(t), & i = j, \\ 0, & i \neq j. \end{cases} \tag{2}$$

where $i, j = 0, 1, \ldots, m-1$.

The other property is orthogonality. It is clear that

$$\int_0^1 \phi_i(t)\phi_j(t)dt = h\delta_{ij}, \tag{3}$$

where δ_{ij} is the Kroneker delta.

The third property is completeness. For every $f \in \mathcal{L}^2([0, 1))$ when m approaches to the infinity, Parseval's identity holds [46]:

$$\int_0^1 f^2(t)dt = \sum_{i=0}^{\infty} f_i^2 \parallel \phi_i(t) \parallel^2, \tag{4}$$

where,

$$f_i = \frac{1}{h} \int_0^1 f(t)\phi_i(t)dt. \tag{5}$$

2.2. Vector Forms

Consider the first m terms of BPFs and write them concisely as m-vector:

$$\Phi(t) = [\phi_0(t), \phi_1(t), \ldots, \phi_{m-1}(t)]^T, \qquad t \in [0, 1) \tag{6}$$

above representation and disjointness property, follows:

$$\Phi(t)\Phi^T(t) = \begin{pmatrix} \phi_0(t) & 0 & \ldots & 0 \\ 0 & \phi_1(t) & \ldots & 0 \\ \vdots & \vdots & \ddots & \vdots \\ 0 & 0 & \ldots & \phi_{m-1}(t) \end{pmatrix}, \tag{7}$$

$$\Phi^T(t)\Phi(t) = 1, \tag{8}$$

$$\Phi(t)\Phi^T(t)V = \tilde{V}\Phi(t), \tag{9}$$

where V is an m-vector and $\tilde{V} = diag(V)$. Moreover, it can be clearly concluded that for every $m \times m$ matrix B:

$$\Phi^T(t)B\Phi(t) = \hat{B}^T\Phi(t), \tag{10}$$

where $\hat{B}$ is an m-vector with elements equal to the diagonal entries of matrix B.

2.3. BPFs Expansion

The expansion of a function $f(t)$ over $[0, 1)$ with respect to $\phi_i(t)$, $i = 0, 1, \ldots, m-1$ may be compactly written as [46]:

$$f(t) \simeq \sum_{i=0}^{m-1} f_i\phi_i(t) = F^T\Phi(t) = \Phi^T(t)F, \tag{11}$$

where $F = [f_0, f_1, \ldots, f_{m-1}]^T$ and f_is are defined by (5).

Now, assume $k(t, s)$ is a function of two variables in $\mathcal{L}^2([0, 1) \times [0, 1))$. It can be similarly expanded with respect to BPFs such as:

$$k(t, s) \simeq \Phi^T(t) K \Psi(s), \tag{12}$$

where $\Phi(t)$ and $\Psi(s)$ are m_1 and m_2 dimensional BPF vectors respectively, and K is the $m_1 \times m_2$ block-pulse coefficient matrix with k_{ij}, $i = 0, 1, \ldots, m-1$, $j = 0, 1, \ldots, m-1$, as follows:

$$k_{ij} = m_1 m_2 \int_0^1 \int_0^1 k(t, s)\ \phi_i(t)\ \psi_j(s) dt ds. \tag{13}$$

For convenience, we can put $m_1 = m_2 = m$.

3. COLLOCATION METHOD USING BLOCK-PULSE BASIS FUNCTIONS

In this section, we extend the definition of BPFs over any interval $[a, b)$. Then, we apply them to solve the integral equations of the second kind by collocation method.

Consider the following Fredholm integral equation of the second kind:

$$x(s) + \int_a^b k(s, t) x(t) dt = y(s) \tag{14}$$

where, $k(s, t)$ and $y(s)$ are known functions but $x(t)$ is unknown. Moreover, $k(s, t) \in \mathcal{L}^2([a, b) \times [a, b))$ and $y(s) \in \mathcal{L}^2([a, b))$. Approximating the function $x(s)$ with respect to BPFs by (11) gives:

$$x(s) \simeq F^T \Phi(s) \tag{15}$$

such that the m-vector F is BPFs coefficients of $x(s)$ that should be determined.

Substituting Eq. (15) into (14) follows:

$$F^T \Phi(s) + F^T \int_a^b k(s, t) \Phi(t) dt \simeq y(s) \tag{16}$$

Now, let s_i, $i = 0, 1, \ldots, m-1$ be m appropriate points in interval $[a, b)$; putting $s = s_i$ in Eq. (16) follows:

$$F^T \Phi(s_i) + F^T \int_a^b k(s_i, t) \Phi(t) dt \simeq y(s_i), \quad i = 0, 1, \ldots, m-1 \tag{17}$$

or:

$$\sum_{j=0}^{m-1} f_j \left[\phi_j(s_i) + \int_a^b k(s_i, t)\phi_j(t)dt\right] \simeq y(s_i), \quad i = 0, 1, \ldots, m-1 \quad (18)$$

Now, replace $\simeq$ with $=$, hence Eq. (18) is a linear system of m algebraic equations for m unknown components $f_0, f_1, \ldots, f_{m-1}$. So, an approximate solution $x(s) \simeq F^T\Phi(s)$, is obtained for Eq. (14).

4. ELECTROMAGNETIC SCATTERING FROM RESISTIVE STRIPS

Now, the problem of determining the scattered electromagnetic fields from resistive strips is solved using the presented approach. In Fig. 1, there is a resistive strip that is very long in the $\pm z$ direction. This strip is encountered by an incoming plane wave that has a polarization with its electric field parallel to the z-axis. The magnetic field of this wave is entirely in the x-y plane, and is therefore transverse to the z-axis. It is called transverse magnetic (TM) polarized wave. This polarization therefore produces a current on the strip that flows along the z-axis.

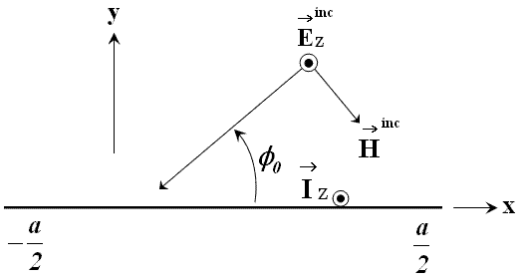

Figure 1. A resistive strip of width a is encountered by an incoming TM-polarized plane wave.

The magnetic vector potential of the current flowing along the strip is given by [48]:

$$A_z = \frac{\mu_0}{4j} \int_{-a/2}^{a/2} I_z(x') H_0^{(2)}(k|x - x'|)dx' \quad (19)$$

where:

$k = \frac{2\pi}{\lambda}$, free space wave number.

λ is the wave length.

$\mu_0 = 4\pi \times 10^{-7}$ H/m, free space permeability.

$G(x, x') = \dfrac{1}{4j} H_0^{(2)}(k|x - x'|)$, 2D free space Green's function.

$H_0^{(2)}(x)$ is a Hankel function of the second kind 0th order.

So, the electric field is given by:

$$E_z(x) = j\omega A_z(x) \tag{20}$$

or

$$E(x) = \frac{\omega\mu_0}{4} \int_{-a/2}^{a/2} I_z(x') H_0^{(2)}(k|x - x'|) dx' \tag{21}$$

Assume that $R_s(x)$ is the surface resistance of the strip and note that the units of surface resistance are in Ω/m^2. The boundary condition at the surface of a thin resistive strip is given by the following equation [48]:

$$-E^{inc} = E^{scat} + R_s(x) J(x) \tag{22}$$

where:

$J(x)$ is the surface current of the strip.

E^{scat} is the scattered electric field produced by the surface current.

Assuming $E^{inc} = e^{jkx\cos\phi_0}$, from Eq. (21) and Eq. (22) it follows:

$$R_s(x) I(x) + \frac{\omega\mu_0}{4} \int_{-a/2}^{a/2} I(x') H_0^{(2)}(k|x - x'|) dx' = -e^{jkx\cos\phi_0} \tag{23}$$

where $I(x)$ is the current of the strip.

Equation (23) can be converted to the following equation:

$$h(x) + \int_a^b G(x, x') h(x') dx' = g(x) \tag{24}$$

where:

$h(x) = I(x)$

$G(x, x') = \dfrac{\omega\mu_0}{4} \dfrac{1}{R_s(x)} H_0^{(2)}(k|x - x'|)$

$g(x) = -\dfrac{1}{R_s(x)} e^{jkx\cos\phi_0}$

It is a Fredholm integral equation of the second kind and can be solved by the presented method. However, from Eq. (23) $I(x)$ can be obtained and then the RCS of the strip can be computed easily.

RCS in two dimensions is defined mathematically as [48]:

$$\sigma(\phi) = \lim_{r\to\infty} 2\pi r \frac{|\mathbf{E}^{scat}|^2}{|\mathbf{E}^{inc}|^2} \tag{25}$$

In two dimensions, the free space Green's function is:

$$G(\mathbf{r},\, \mathbf{r}') = \frac{1}{4j} H_0^{(2)}(k|\mathbf{r} - \mathbf{r}'|) \tag{26}$$

The magnetic vector potential in two-dimensional space is:

$$\mathbf{A}(\mathbf{r}) = \mu \int\int \mathbf{J}(\mathbf{r}') G(\mathbf{r},\, \mathbf{r}') ds' \tag{27}$$

The electric field is given by:

$$\mathbf{E} = j\omega \mathbf{A} \tag{28}$$

Combining (26), (27), and (28) we obtain:

$$\mathbf{E}(\mathbf{r}) = \frac{\omega\mu}{4} \int\int \mathbf{J}(\mathbf{r}') H_0^{(2)}(k|\mathbf{r} - \mathbf{r}'|) ds' \tag{29}$$

In the TM situation, the incident electric field along the strip is $1\,\mathrm{V/m}$ ($|\mathbf{E}^{inc}|^2 = 1$). So, the denominator of Eq. (25) is unity. This allows us to turn our attention to the numerator. To evaluate (29), we note that as $r \longrightarrow \infty$, we can use the large argument approximation for the Hankel function [48]:

$$H_0^{(2)}(r) \approx \sqrt{\frac{2}{\pi r}} e^{-j(r - \frac{\pi}{4})} \tag{30}$$

Substituting this into (29) and implementing Eq. (25) for the TM case, we obtain:

$$\sigma(\phi) = \frac{k\eta^2}{4} \left| \int_{strip} I(x',\, y') e^{jk(x'\cos\phi + y'\sin\phi)} dl' \right|^2 \tag{31}$$

where $\eta = 376.73\,\Omega$.

In the presented case, the strip is restricted to the x-axis, which simplifies Eq. (31):

$$\sigma(\phi) = \frac{k\eta^2}{4} \left| \int_{-a/2}^{a/2} I(x') e^{jkx'\cos\phi} dx' \right|^2 \tag{32}$$

Also, it is possible to define a logarithmic quantity with respect to the RCS, so that:

$$\sigma_{dBlm} = 10 \log_{10} \sigma \tag{33}$$

4.1. Uniform Resistance Distribution

Assume that the $R_s(x)$ has a uniform value in throughout of the surface of strip. Considering Eq. (23), $I(x)$ is computed for R_s of 0, 500, $1000\,(\Omega/\mathrm{m}^2)$, $\phi_0 = \frac{\pi}{2}$, $a = 6\lambda\,(\mathrm{m})$ and $f = 0.3\,\mathrm{GHz}$, and then RCS is obtained of Eqs. (32) and (33). The current distributions of the resistive strip for these values of R_s are shown in Figs. 2–5.

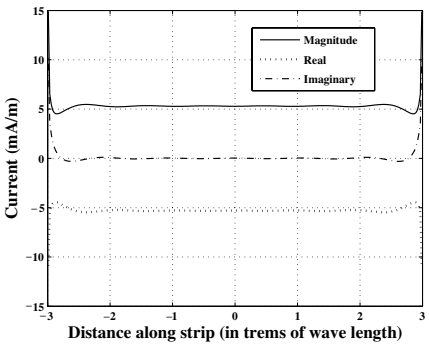

Figure 2. Current distribution across a $6-\lambda$ strip created by a TM-polarized plane wave for $R_s = 0$ and $f = 0.3\,\mathrm{GHz}$.

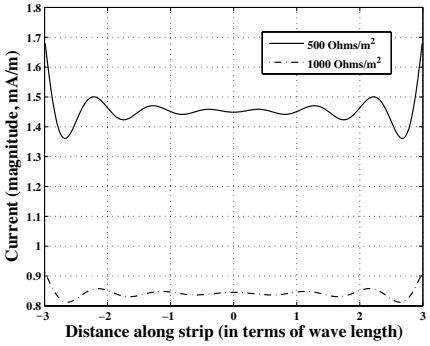

Figure 3. Current magnitude across the $6-\lambda$ resistive strip for R_s of 500 and $1000\,(\Omega/\mathrm{m}^2)$ and $f = 0.3\,\mathrm{GHz}$.

In Figs. 6 and 7, the bistatic RCS of the $6-\lambda$ resistive strip, for R_s of 0, 500, $1000\,(\Omega/\mathrm{m}^2)$ and for $\phi_0 = \frac{\pi}{2}$, $\frac{2\pi}{3}$ has been shown. Also, in Fig. 8 the monostatic RCS of this strip is given. It is seen that the level of the first side lobe is nearly 13 dB down from the main lobe.

4.2. Quadratic Resistive Taper

Consider a quadratic resistive taper expressed by:

$$R_s(x) = 2\eta \left(\frac{kx}{a}\right)^2 \qquad (\Omega/\mathrm{m}^2) \tag{34}$$

where, k is a real constant value.

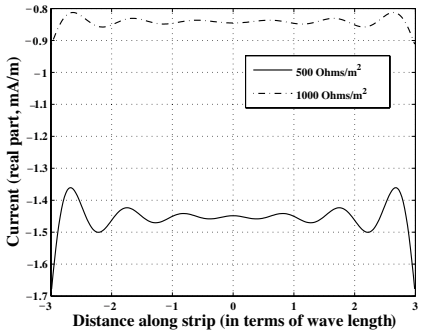

Figure 4. The real part of current across the $6-\lambda$ resistive strip for R_s of 500 and 1000 (Ω/m^2) and $f = 0.3\,\mathrm{GHz}$.

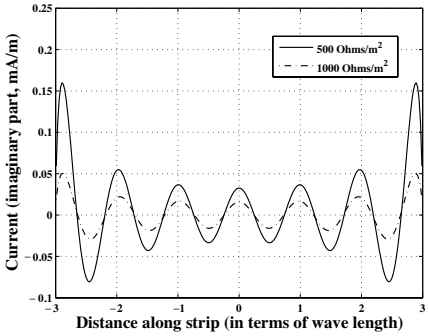

Figure 5. The imaginary part of current across the $6-\lambda$ resistive strip for R_s of 500 and 1000 (Ω/m^2) and $f = 0.3\,\mathrm{GHz}$.

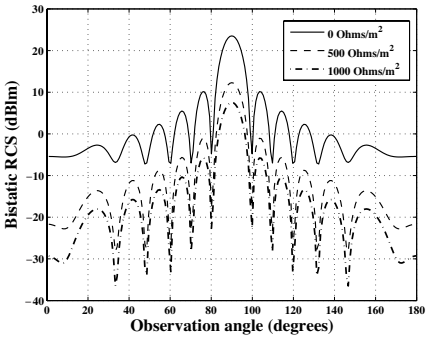

Figure 6. The bistatic RCS of the $6-\lambda$ resistive strip for R_s of 0, 500, 1000 (Ω/m^2) and $\phi_0 = \frac{\pi}{2}$.

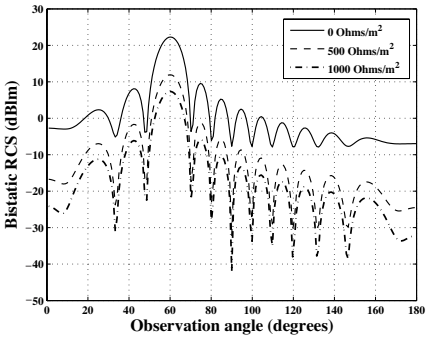

Figure 7. The bistatic RCS of the $6-\lambda$ resistive strip for R_s of 0, 500, 1000 (Ω/m^2) and $\phi_0 = \frac{2\pi}{3}$.

Figure 9 shows the quadratic taper of a $6-\lambda$ strip for $k = 2$. After computing $I(x)$ by Eq. (23), the RCS of this strip can be obtained. For $\phi_o = \frac{\pi}{2}$, the magnitude, real part and imaginary part of strip current are shown in Figs. 10 and 11, and the bistatic radar cross section of this strip shown in Figs. 12 and 13 has been calculated for $k = 0.5,\ 1,\ 2$, $\phi_0 = \frac{\pi}{2},\ \frac{\pi}{4}$, and $f = 0.3\,\mathrm{GHz}$. Fig. 14 shows the monostatic RCS. It is seen that the quadratic taper reduces the first side lobe to a level of $-23\,\mathrm{dB}$ below the main lobe. This taper has reduced the first side lobe by $10\,\mathrm{dB}$, compared with a uniform distribution.

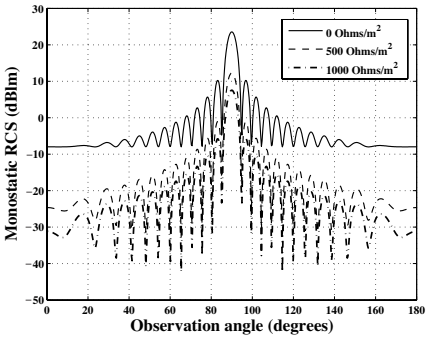

Figure 8. The monostatic RCS of the $6-\lambda$ resistive strip for R_s of 0, 500, 1000 (Ω/m^2).

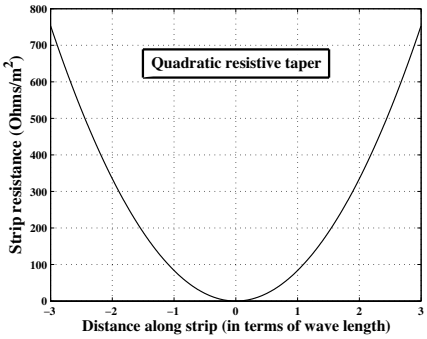

Figure 9. The quadratic taper of a $6-\lambda$ resistive strip for $k=2$.

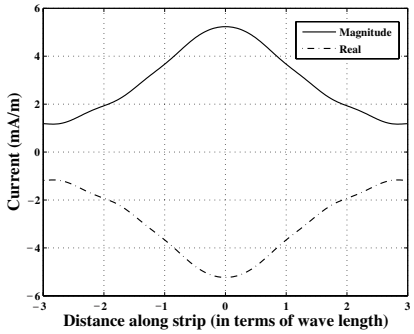

Figure 10. The magnitude and real part of current across the $6-\lambda$ resistive strip of Fig. 9 for $k=2$ and $f=0.3\,\mathrm{GHz}$.

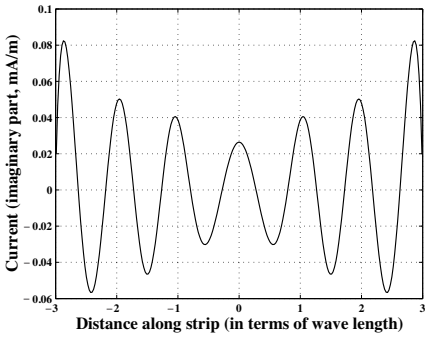

Figure 11. The imaginary part of current across the $6-\lambda$ resistive strip of Fig. 9 for $k=2$ and $f=0.3\,\mathrm{GHz}$.

4.3. Sinc form Resistance Distribution

In this subsection the problem of determining the scattered fields is solved for a resistive strip of a sinc form resistance distribution shown in Fig. 15.

Consider a sinc form resistance expressed by:

$$R_s(x) = 2\eta \left| \frac{\sin k\pi a x}{k\pi a x} \right| \qquad (\Omega/\mathrm{m}^2) \tag{35}$$

in which, k is a real constant value.

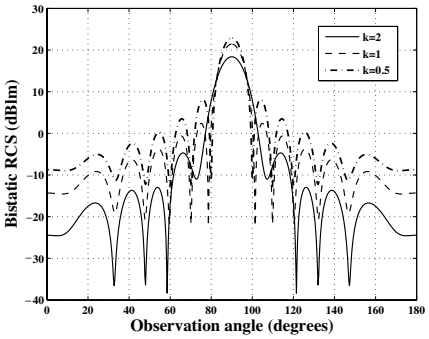

Figure 12. The bistatic RCS of the $6-\lambda$ resistive strip of Fig. 9 for $k = 0.5,\ 1,\ 2$ and $\phi_0 = \frac{\pi}{2}$.

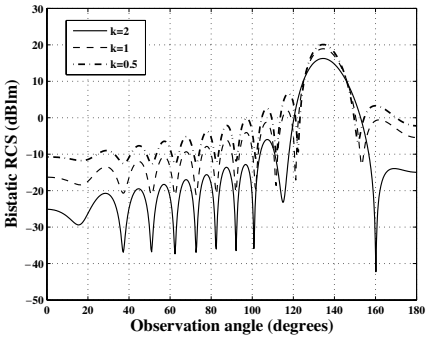

Figure 13. The bistatic RCS of the $6-\lambda$ resistive strip of Fig. 9 for $k = 0.5,\ 1,\ 2$ and $\phi_0 = \frac{\pi}{4}$.

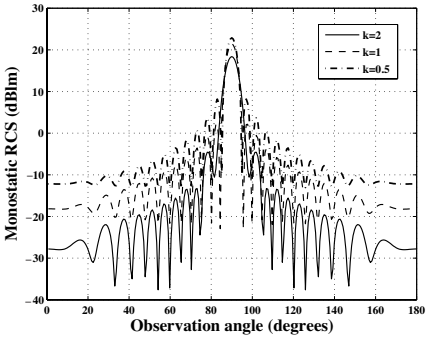

Figure 14. The monostatic RCS of the $6-\lambda$ resistive strip of Fig. 9 for $k = 0.5,\ 1,\ 2$.

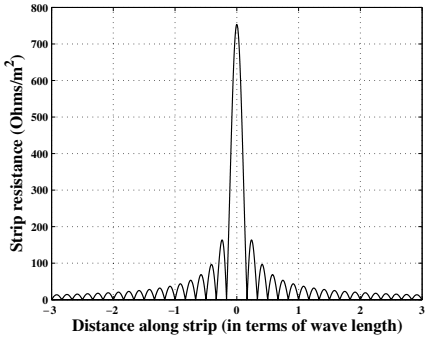

Figure 15. Sinc form resistance distribution of a $6-\lambda$ resistive strip for $k = 1$.

Applying Eq. (23) to this case gives the current distribution which has been shown in Fig. 16. Then, the bistatic RCS of this case is obtained of Eqs. (32) and (33). Fig. 17 shows the results for $k = 0.8$, 3, 30 and $f = 0.3\,\text{GHz}$.

For $k = 30$, the level of the first side lobe is nearly 13 dB down from the main lobe.

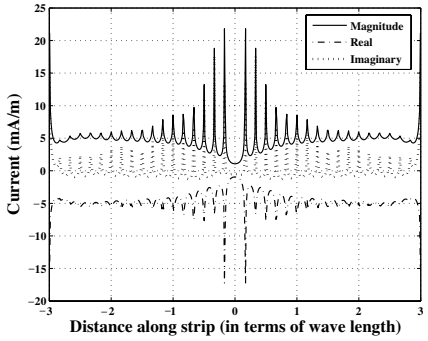

Figure 16. Current across the $6-\lambda$ resistive strip of Fig. 15 for $k=1$ and $f=0.3\,\mathrm{GHz}$.

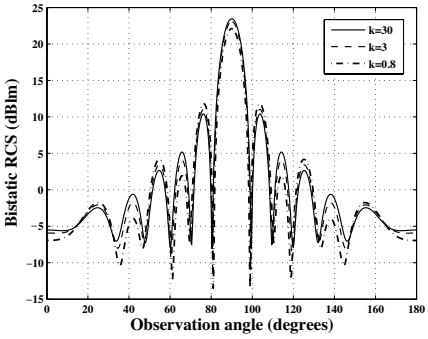

Figure 17. The bistatic RCS of the $6-\lambda$ resistive strip of Fig. 15 for $k=0.8$, 3, 30 and $\phi_0=\frac{\pi}{2}$.

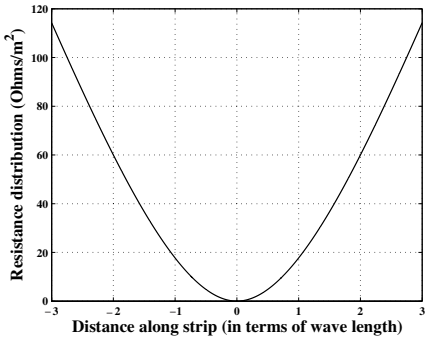

Figure 18. Exponential resistance distribution of a $6-\lambda$ resistive strip for $k=1$.

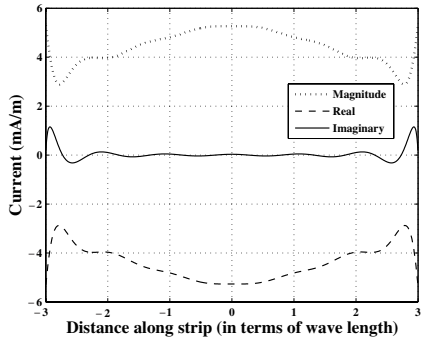

Figure 19. Current across the $6-\lambda$ resistive strip of Fig. 18 for $k=1$ and $f=0.3\,\mathrm{GHz}$.

4.4. Exponential Distribution

The final case is an exponential form distribution of the strip resistance which is defined below:

$$R_s(x)=2\eta\left(\frac{kx}{a}\right)^2\exp\left(-\left|\frac{kx}{a}\right|\right)\qquad(\Omega/\mathrm{m}^2)\tag{36}$$

Figure 18 shows the exponential form resistance distribution of a $6-\lambda$ strip for $k=1$. Current distribution of this case for $k=1$ is shown in Fig. 19, and its bistatic RCS for $k=0.5$, 1, 1.5 and $f=0.3\,\mathrm{GHz}$ is shown in Fig. 20.

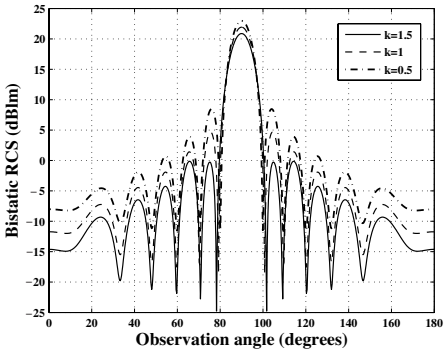

Figure 20. The bistatic RCS of the $6-\lambda$ resistive strip of Fig. 18 for $k = 0.5,\ 1,\ 1.5$ and $\phi_0 = \frac{\pi}{2}$.

5. DISCUSSION ON THE RESULTS

Here, we discuss on both the current distributions and the RCSs.

5.1. Current Distributions

Figures 2–5 show the current distribution across the strip for R_s of 0, 500, 1000 (Ω/m^2). It is seen that the current distribution across the all strips approaches to infinity at the edges, but it has less extreme oscillations across the resistive cases ($R_s = 500, 1000\,(\Omega/\mathrm{m}^2)$), and the variations amplitude decreases by rising R_s. So, for the uniform distribution, increasing in R_s causes the current to be less oscillatory, and on the other hand causes the current magnitude to decrease.

For the quadratic resistive taper, the current distribution has a finite value at the edges contrary to the uniform distribution. It seems to be due to the high impedance at the edges in comparison with the uniform distribution. Fig. 10 shows that the magnitude and real part of the current have a maximum value that occurs in the middle of the strip. But the imaginary part of the current has a quite different behavior by comparison the magnitude and real part. It is seen that the imaginary part is extremely oscillatory.

Figure 16 shows that the magnitude, real part and imaginary part of the current created on the strip of the sinc form resistance has many oscillations that is due to the numerous variations in the resistance distribution which corresponds with the sinc function. Also, the current value approaches to infinity at the edges, because the value of the sinc function approaches to zero at the edges.

For the exponential form distribution, the magnitude and real part

of the current have a local maximum in the middle of the strip. Also, it is seen that the current value is enlarged at the edges (more than of the quadratic resistive taper), but it is less than of the uniform and sinc form distributions.

5.2. RCSs

Considering Figs. 6 and 8, it can be seen that for uniform distribution, increasing in surface resistance in both bistatic and monostatic RCS only causes the levels of main lobe and side lobes to decrease, but the maximum (relative) side lobe level (SLL) doesn't change. SLL value for this case is about -13 dB for any value of the surface resistance and for both bistatic and monostatic RCS.

For the quadratic resistive taper, the main lobe and side lobes

Table 1. Summary of discussions.

Resistance distribution	$0.5 \leq k \leq 1.5$		$1.5 < k \leq 10$	
	$k \uparrow$	$k \downarrow$	$k \uparrow$	$k \downarrow$
Uniform	- -	- -	- -	- -
Quadratic taper	MLL↓ SLL↓	MLL↑ SLL↑	MLL↓ SLL↓	MLL↑ SLL↑
Sinc form	MLL↑ SLL↓	MLL↓ SLL↑	MLL↑ SLL↓	MLL↓ SLL↑
Exponential form	MLL↓ SLL↓	MLL↑ SLL↑	- -	- -

Resistance distribution	$k > 10$		For uniform	
	$k \uparrow$	$k \downarrow$	$R_s \uparrow$	$R_s \downarrow$
Uniform	- -	- -	MLL↓ -	MLL↑ -
Quadratic taper	MLL↓ SLL↓	MLL↑ SLL↑	- -	- -
Sinc form	- SLL↓	- SLL↑	- -	- -
Exponential form	- -	- -	- -	- -

levels increase when k decreases (see Figs. 12 and 14); Also, SLL increases (in both bistatic and monostatic RCS). So, increasing k causes SLL to decrease. The SLL value for $k = 2$ is nearly $-23\,\mathrm{dB}$ and it can be seen that this taper reduces the first side lobe by 10 dB, compared with a uniform distribution.

Figure 17 shows that for the sinc form resistance distribution, SLL value decreases with increasing k, but the main lobe level increases. So, using the sinc form distribution we can simultaneously obtain a low SLL and a main lobe with high level when k increases. For $k > 10$, the main lobe level doesn't have considerable changes, but SLL becomes more and more less when k increases, because the side lobe level decreases. The SLL value for $k = 30$ is nearly $-13\,\mathrm{dB}$.

The exponential form resistance distribution behaves like quadratic taper for $0.5 \leq k \leq 1.5$ (see Fig. 20), but it has another behavior for other values of k. The SLL value for $k = 1.5$ is about $-21\,\mathrm{dB}$.

A summary of the discussions posed in this subsection has been presented in Table 1. Note that MLL means "main lobe level".

6. CONCLUSION

The presented method in this paper is applied to solve the integral equations of the second kind arising in problem of determining the scattered electromagnetic fields from resistive strips.

As the numerical results showed, this method reduces an integral equation of the second kind to a linear system of algebraic equations.

The problem of electromagnetic scattering from resistive strips was treated in detail, and an extensive discussion on the obtained results was performed.

This method can be easily generalized to apply to objects of arbitrary geometry and arbitrary material.

REFERENCES

1. Wilton, D. R. and C. M. Butler, "Effective methods for solving integral and integro-differential equations," *Electromagnetics*, Vol. 1, 289–308, 1981.
2. Harrington, R. F., "Matrix methods for field problems," *Proc. IEEE*, Vol. 55, No. 2, 136–149, 1967.
3. Mishra, M. and N. Gupta, "Monte Carlo integration technique for the analysis of electromagnetic scattering from conducting surfaces," *Progress In Electromagnetics Research*, PIER 79, 91–106, 2008.

4. Arnold, M. D., "An efficient solution for scattering by a perfectly conducting strip grating," *Journal of Electromagnetic Waves and Applications*, Vol. 20, No. 7, 891–900, 2006.
5. Zhao, J. X., "Numerical and analytical formulations of the extended MIE theory for solving the sphere scattering problem," *Journal of Electromagnetic Waves and Applications*, Vol. 20, No. 7, 967–983, 2006.
6. Ruppin, R., "Scattering of electromagnetic radiation by a perfect electromagnetic conductor sphere," *Journal of Electromagnetic Waves and Applications*, Vol. 20, No. 12, 1569–1576, 2006.
7. Ruppin, R., "Scattering of electromagnetic radiation by a perfect electromagnetic conductor cylinder," *Journal of Electromagnetic Waves and Applications*, Vol. 20, No. 13, 1853–1860, 2006.
8. Hussein, K. F. A., "Efficient near-field computation for radiation and scattering from conducting surfaces of arbitrary shape," *Progress In Electromagnetics Research*, PIER 69, 267–285, 2007.
9. Hussein, K. F. A., "Fast computational algorithm for EFIE applied to arbitrarily-shaped conducting surfaces," *Progress In Electromagnetics Research*, PIER 68, 339–357, 2007.
10. Kishk, A. A., "Electromagnetic scattering from composite objects using a mixture of exact and impedance boundary conditions," *IEEE Transactions on Antennas and Propagation*, Vol. 39, No. 6, 826–833, 1991.
11. Caorsi, S., A. Massa, and M. Pastorino, "A numerical solution to full-vector electromagnetic scattering by three-dimensional nonlinear bounded dielectrics," *IEEE Transactions on Microwave Theory and Techniques*, Vol. 43, No. 2, 428–436, 1995.
12. Shore, R. A. and A. D. Yaghjian, "Dual-surface integral equations in electromagnetic scattering," *IEEE Transactions on Antennas and Propagation*, Vol. 53, No. 5, 1706–1709, 2005.
13. Ylä-Oijala, P. and M. Taskinen, "Well-conditioned Müller formulation for electromagnetic scattering by dielectric objects," *IEEE Transactions on Antennas and Propagation*, Vol. 53, No. 10, 3316–3323, 2005.
14. Li, L. W., P. S. Kooi, Y. L. Qin, T. S. Yeo, and M. S. Leong, "Analysis of electromagnetic scattering of conducting circular disk using a hybrid method," *Progress In Electromagnetics Research*, PIER 20, 101–123, 1998.
15. Liu, Y. and K. J. Webb, "On detection of the interior resonance errors of surface integral boundary conditions for electromagnetic scattering problems," *IEEE Transactions on Antennas and*

Propagation, Vol. 49, No. 6, 939–943, 2001.

16. Kishk, A. A., "Electromagnetic scattering from transversely corrugated cylindrical structures using the asymptotic corrugated boundary conditions," *IEEE Transactions on Antennas and Propagation*, Vol. 52, No. 11, 3104–3108, 2004.
17. Tong, M. S. and W. C. Chew, "Nystrom method with edge condition for electromagnetic scattering by 2D open structures," *Progress In Electromagnetics Research*, PIER 62, 49–68, 2006.
18. Valagiannopoulos, C. A., "Closed-form solution to the scattering of a skew strip field by metallic pin in a slab," *Progress In Electromagnetics Research*, PIER 79, 1–21, 2008.
19. Frangos, P. V. and D. L. Jaggard, "Analytical and numerical solution to the two-potential Zakharov-Shabat inverse scattering problem," *IEEE Transactions on Antennas and Propagation*, Vol. 40, No. 4, 399–404, 1992.
20. Barkeshli, K. and J. L. Volakis, "Electromagnetic scattering from thin strips — Part II: Numerical solution for strips of arbitrary size," *IEEE Transactions on Education*, Vol. 47, No. 1, 107–113, 2004.
21. Collino, F., F. Millot, and S. Pernet, "Boundary-integral methods for iterative solution of scattering problems with variable impedance surface condition," *Progress In Electromagnetics Research*, PIER 80, 1–28, 2008.
22. Zahedi, M. M. and M. S. Abrishamian, "Scattering from semi-elliptic channel loaded with impedance elliptical cylinder," *Progress In Electromagnetics Research*, PIER 79, 47–58, 2008.
23. Zaki, K. A. and A. R. Neureuther, "Scattering from a perfectly conducting surface with a sinusoidal height profile: TE polarization," *IEEE Transactions on Antennas and Propagation*, Vol. 19, No. 2, 208–214, 1971.
24. Carpentiery, B., "Fast iterative solution methods in electromagnetic scattering," *Progress In Electromagnetics Research*, PIER 79, 151–178, 2008.
25. Du, Y., Y. L. Luo, W. Z. Yan, and J. A. Kong, "An electromagnetic scattering model for soybean canopy," *Progress In Electromagnetics Research*, PIER 79, 209–223, 2008.
26. Umashankar, K. R., S. Nimmagadda, and A. Taflove, "Numerical analysis of electromagnetic scattering by electrically large objects using spatial decomposition technique," *IEEE Transactions on Antennas and Propagation*, Vol. 40, No. 8, 867–877, 1992.

27. Gokten, M., A. Z. Elsherbeni, and E. Arvas, "Electromagnetic scattering analysis using the two-dimensional MRFD formulation," *Progress In Electromagnetics Research*, PIER 79, 387–399, 2008.
28. Hatamzadeh-Varmazyar, S., M. Naser-Moghadasi, and Z. Masouri, "A moment method simulation of electromagnetic scattering from conducting bodies," *Progress In Electromagnetics Research*, PIER 81, 99–119, 2008.
29. Hatamzadeh-Varmazyar, S. and M. Naser-Moghadasi, "New numerical method for determining the scattered electromagnetic fields from thin wires," *Progress In Electromagnetics Research B*, Vol. 3, 207–218, 2008.
30. Hatamzadeh-Varmazyar, S. and M. Naser-Moghadasi, "An integral equation modeling of electromagnetic scattering from the surfaces of arbitrary resistance distribution," *Progress In Electromagnetics Research B*, Vol. 3, 157–172, 2008.
31. Abd-El-Ranouf, H. E. and R. Mittra, "Scattering analysis of dielectric coated cones," *Journal of Electromagnetic Waves and Applications*, Vol. 21, No. 13, 1857–1871, 2007.
32. Choi, S. and N.-H. Myung, "Scattering analysis of open-ended cavity with inner object," *Journal of Electromagnetic Waves and Applications*, Vol. 21, No. 12, 1689–1702, 2007.
33. Li, Y.-L., J.-Y. Huang, and S.-H. Gong, "The scattering cross section for a target irradiated by time-varying electromagnetic waves," *Journal of Electromagnetic Waves and Applications*, Vol. 21, No. 9, 1265–1271, 2007.
34. Rui, P.-L. and R. Chen, "Implicity restarted gmres fast Fourier transform method for electromagnetic scattering," *Journal of Electromagnetic Waves and Applications*, Vol. 21, No. 7, 973–976, 2007.
35. Nicolic, N., J. S. Kot, and S. Vinogradov, "Scattering by a luneberg lens partially covered by a metallic cap," *Journal of Electromagnetic Waves and Applications*, Vol. 21, No. 4, 549–563, 2007.
36. Yuan, H.-W., S.-X. Gong, X. Wang, and W.-T. Wang, "Scattering analysis of a printed dipole antenna using PBG structures," *Progress In Electromagnetics Research B*, Vol. 1, 189–195, 2008.
37. Faghihi, F. and H. Heydari, "A combination of time domain finite element-boundari integral and with time domain physical optics for calculation of electromagnetic scattering of 3-D structures," *Progress In Electromagnetics Research*, PIER 79, 463–474, 2008.

38. Ahmed, S. and Q. A. Naqavi, "Electromagnetic scattering from a perfect electromagnetic conductor cylinder buried in a dielectric half-space," *Progress In Electromagnetics Research*, PIER 78, 25–38, 2008.
39. Valagiannopoulos, C. A., "Electromagnetic scattering from two eccentric metamaterial cylinders with frequency-dependent permittivities differing slightly each other," *Progress In Electromagnetics Research B*, Vol. 3, 23–34, 2008.
40. Hady, L. K. and A. A. Kishk, "Electromagnetic scattering from conducting circular cylinder coated by meta-materials and loaded with helical strips under oblique incidence," *Progress In Electromagnetics Research B*, Vol. 3, 189–206, 2008.
41. Zainud-Deen, S. H., A. Z. Botros, and M. S. Ibrahim, "Scattering from bodies coated with metamaterial using FDFD method," *Progress In Electromagnetics Research B*, Vol. 2, 279–290, 2008.
42. Li, Y.-L., J.-Y. Huang, M.-J. Wang, and J. Zhang, "Scattering field for the ellipsoidal targets irradiated by an electromagnetic wave with arbitrary polarizing and propagating direction," *Progress In Electromagnetics Research Letters*, Vol. 1, 221–235, 2008.
43. Balanis, C. A., *Advanced Engineering Electromagnetics*, Wiley, New York, 1989.
44. Balanis, C. A., *Antenna Theory: Analysis and Design*, Wiley, New York, 1982.
45. Delves, L. M. and J. L. Mohamed, *Computational Methods for Integral Equations*, Cambridge University Press, Cambridge, 1985.
46. Babolian, E. and Z. Masouri, "Direct method to solve Volterra integral equation of the first kind using operational matrix with block-pulse functions," *Journal of Computational and Applied Mathematics*, in press, doi: 10.1016/j.cam.2007.07.029, 2007.
47. Babolian, E. and A. Salimi Shamloo, "Numerical solution of Volterra integral and integro-differential equations of convolution type by using operational matrices of piecewise constant orthogonal functions," *Journal of Computational and Applied Mathematics*, in press, doi: 10.1016/j.cam.2007.03.007, 2007.
48. Bancroft, R., *Understanding Electromagnetic Scattering Using the Moment Method*, Artech House, London, 1996.